High yield vesicle packaged recombinant protein production from *E. coli.*

Tara A. Eastwood[1], Karen Baker[1], Bree R. Streather[1], Nyasha Allen[1,2], Lin Wang[3], Stanley W. Botchway[3], Ian R. Brown[1], Jennifer R. Hiscock[2], Christopher Lennon[4] and Daniel P. Mulvihill[1]*

[1] School of Biosciences, University of Kent, Canterbury, Kent, CT2 7NJ, UK.

[2] School of Chemistry and Forensics, University of Kent, Canterbury, Kent, CT2 7NJ, UK.

[3] Central Laser Facility, Research Complex at Harwell, Science and Technology Facilities Council, Rutherford Appleton Laboratory, Harwell, Didcot, Oxford, OX11 0QX, UK.

[4] Fujifilm-Diosynth Biotechnologies UK Ltd, Belasis Avenue, Billingham, TS23 1LH, UK.

* Corresponding author and Lead contact. email - d.p.mulvihill@kent.ac.uk

https://orcid.org: TAE: 0000-0003-2587-0574; KB: 0000-0001-7628-1978; BRS: 0000-0003-0190-8558; NA: 0000-0002-9971-6118; LW: 0000-0001-9141-5217; SWB: 0000-0002-3268-9303; IRB: 0000-0002-6989-4474; JRH: 0000-0002-1406-8802; CL: 0000-0002-2437-1485; DPM: 0000-0003-2502-5274.

SUMMARY

We describe an innovative system that exports diverse recombinant proteins in membrane bound vesicles from *E. coli*. These recombinant vesicles compartmentalise proteins within a micro-environment that allows production of otherwise challenging insoluble, toxic, or disulphide-bond containing proteins from bacteria. The release of the inducible vesicle packaged soluble protein supports isolation from the culture within an environment allowing long term storage of active protein. This technology results in high-yields of vesicle packaged soluble functional proteins for efficient downstream processing for a wide range of applications from discovery science to applied biotechnology and medicine.

MOTIVATION

The ability to reprogram a cell to direct the packaging of specific molecules into discrete membrane envelopes is a major objective for synthetic biology. The ability to export proteins from the *E. coli* not only simplifies the subsequent protein purification, but the controlled packaging into membrane vesicles supports the development of numerous technologies and commercialisable products within the applied biotechnology and medical industries, including: generation of recombinant bioreactors; environmental dispersion of biomolecules; vehicles for drug delivery and vaccination, as well as providing a stable environment for isolation and storage of proteins.

INTRODUCTION

Recombinant protein production has led to a revolution in basic research, biotechnology and biotherapeutic industries, and plays a key role in treatment of a wide range of major diseases. Currently, the majority of commercial recombinant protein is produced using either bacterial or eukaryotic cell expression systems, dependent upon the structural complexity and cell dependent modifications required to obtain functional protein. The Gram-negative bacteria, *E. coli*, is an attractive system for recombinant protein production in both academic and industrial scales. It is not only cheap and easy to culture in batches to high densities, but a wide range of strains, reagents, promoters and tools have been developed to facilitate the production

of functional proteins in *E. coli*. In addition, the application of synthetic biology strategies are now overcoming limitations commonly associated with the application of post-translational modifications and folding of complex proteins.[1]

Here we describe an innovative expression system that induces packaging of a diverse range of recombinant proteins into membrane vesicles in *E. coli*. This simple peptide tag-based technology results in high-yields of vesicle packaged soluble proteins, that allows compartmentalisation of otherwise toxic, insoluble and disulphide bond containing proteins, as well as extracellular release of vesicles into the media for efficient downstream processing. These released protein-packed vesicles support rapid isolation from the media and also provide a micro-environment for stable long-term storage of functional recombinant proteins. Thus this system provides significant benefit for a wide range of applications from discovery science to applied biotechnology and medicine.

RESULTS

During the development of a fluorescence based drug screen to identify effectors of alpha-synuclein oligomerisation [2], we serendipitously discovered that recombinant expression of full-length human α-synuclein (αSyn) in *E. coli* brought about the release of extracellular αSyn containing membrane vesicles, frequently containing the bacterial membrane protein, OmpA (Fig. 1a). Further analysis revealed the alpha-helical [3] amino-terminal 38 residues of αSyn is sufficient to bring about the formation and release of OmpA labelled extracellular membrane bound vesicles from *E. coli* cells into the culture media (Fig. 1b). *In vitro* analysis revealed this αSyn derived polypeptide, named here "Vesicle Nucleating peptide" (VNp), interacts with vesicles composed of reconstituted *E. coli* membrane lipids, and subsequently stabilise its alpha-helical structure [4] (Supplementary Fig. 1). FLIM-FRET revealed the VNp-fusion specifically associates with the inner *E. coli* membrane *in vivo* (Supplementary Fig. 1), which coincides with the formation and release of recombinant VNp containing vesicles into the growth media (Fig. 1 a, c-e). This process occurs without impacting cell growth and so drives large-scale production of vesicles from cells (Fig. 1e, Supplementary Fig. 1) to support isolation of recombinant proteins from growth culture media, as well as from cells harvested upon termination of the culture, thus providing significant savings in both time and resource.

Fusion of sequences encoding VNp to those encoding the monomeric fluorescent protein mNeongreen [5] led to the production and export of large VNp-mNeongreen protein vesicles into the culture media (Fig. 1 f-g). Immuno-electron microscopy confirmed the exclusive localisation of the mNeongreen cargo within the lumen of the vesicles (Fig. 1g, Supplementary Fig. 2). Low speed centrifugation and subsequent filtration with sterile 0.45 µm polyethersulfone (PES) filters efficiently and effectively isolated the vesicles from bacteria (Fig. 1h-i, Supplementary Fig. 2). Average polydispersity indices from dynamic light scattering (DLS) analysis of isolated VNp induced vesicles were greater than 1, indicating vesicles with a broad distribution of sizes in the culture media. There was no significant difference in the zeta potential (calculated from peak maxima) between day old (-10.5 mV) and 4 month old vesicles (-11.1 mV), and no observable significant loss in vesicle contained VNp-mNeongreen from vesicles over a 3 month period (Supplementary Fig. 2). Thus the isolated vesicles provide a stable environment for effective long term protein storage of soluble recombinant protein (Supplementary Fig. 2). The degree of purity of the fusion protein harvested by one step filtration was determined by mass spectroscopic protein analysis of the isolated vesicles, and was found to be sufficient for a very wide range of applications (Fig. 1i, Supplementary Fig. 2), while simultaneously supporting subsequent purification after vesicle sonication, where necessary. Together these data support a model of the VNp-fusion interacting with the *E. coli* membrane, and subsequent incorporation into vesicles that release into the culture media (Fig. 1j).

This system provides a simple and attractive mechanism for releasing membrane packaged recombinant proteins into the media enabling both enhanced recombinant protein production and subsequent processing. While mNeongreen provided rapid quantification of soluble target protein exported into the media, a wider range of proteins, including a number of model biopharmaceuticals, representing a range of different physical properties and expression challenges (such as membrane binding, disulphide-bond containing, or otherwise insoluble or toxic proteins – see Supplementary Information) were used to test the applicability of this technology for the expression of the spectrum of molecules demanded by the life sciences community. Expression of each protein was tested as VNp, or VNp-mNeongreen amino terminal fusions and compared to the expression of equivalent non-VNp fusion proteins (Fig. 1 k-m, Table 1, Supplementary Fig. 2).

The VNp fusion enhanced the expression of each target protein highly effectively, and supports the expression of individual proteins ranging from less than 1 kDa (VNp-His6) to 85 kDa (VNp-mNeongreen-Etanercept) in size, as well as protein complexes as demonstrated by fluorescence from pairs of Bimolecular Fluorescence Complementation (BiFC) VNp-fusions [6] within exported vesicles (Supplementary Fig. 3). Importantly, VNp fusion enhanced the overall yield of each target protein examined, with yields of almost 1g soluble protein / litre of shaking flask culture obtained in the case for the Designed Ankyrin Repeat protein, DARPin Off7 (DARP) (Table 1). Interestingly while the addition of the mNeongreen tag was seen to enhance the expression of solubility EPO, Etanercept and hGH, the addition of the 25 kDa mNeongreen fluorescent protein tag resulted in a reduction in the overall yield of each model therapeutic protein examined. This is likely to be due to a combinantion of an overall increase in protein size, as well as a varying negative effect mNeongreen can have on the growth of the bacterial cell (Supplementary Fig. 1). In addition, we observed no significant variation in the size or abundance of the VNp induced vesicles from cultures expressing different VNp-fusions, therefore the differences in abundances (Table 1) are likely due to differences in expression and packaging efficiency within the vesicle. Tobacco Etch Virus (TEV) protease cleavage of the VNp-mNeongreen tag from VNp-mNeongreen-TEV-DARP and VNp-mNeongreen-TEV-Uricase did not impact the solubility of the resultant purified DARP and Uricase proteins (Supplementary Fig. 3), indicating that once expressed the VNp tag is not necessary for maintaining protein solubility.

The VNp expression system was further validated by illustrating its application to larger volume fermentation cultures (Supplementary Fig. 3). VNp-DARP expression was induced in *E. coli* over a 24 hr period within 15L fermentation vessels (see materials and methods for details). Not only was expression and export of the VNp-DARP fusion sustained over the 24 hr period (Supplementary Fig. 3), yields of VNp-DARP protein greater than 1.4 g/ L were reproducibly obtained, which represented 65 % of total protein observed within the cleared medium fraction.

The versatility of the system was further demonstrated by the production of correctly folded (e.g. mNeongreen,), membrane binding (FGF21), as well as enzymatically active (uricase) proteins (Supplementary Fig. 3). The vesicle isolated VNp-uricase was

not only as enzymatically active as uricase purified from a cell pellet, but this activity was maintained to a higher degree by VNp-uricase stored within isolated vesicles for 2 months at 4 ºC when compared to purified protein stored at 4 ºC in buffer over the same period (Supplementary Fig. 3), highlighting the stable environment the vesicles afford their protein cargo.

The VNp fusion allows production of soluble proteins that are otherwise insoluble or reduce the viability of bacterial cells (e.g. DNase, Etanercept, Erythropoietin (EPO) & human Growth Hormone (hGH)) (Table 1, Supplementary Fig. 3). In the case of the disulphide bond containing proteins Etanercept and hGH,[7,8] the majority of the soluble recombinant protein remained within the cell (Table 1). EM data show fusing VNp-mNG to Etanercept, an anti-inflamatory therapeutic consisting of a fusion between a Tumour Necrosis Factor and IgG1, impacts VNp remodelling of the inner membrane to induce VNp-fusion containing internalised cytosolic membrane structures (Fig. 2a-b). This TNF-IgG1 therapeutic fusion was not only dimeric (disulphide-bond dependent), but also exhibited appropriate ligand binding properties when isolated from VNp induced cytosolic vesicles. The ability to bind protein A was maintained upon TEV protease dependent proteolytic removal of the VNp-mNeongreen fusion (Fig. 2c-e). Similarly, proteolytic cleavage of VNp-mNG from VNp-mNG-TEV-DARP and VNp-mNG-TEV-Uricase did not impact the solubility of DARP or Uricase (Fig. 2f), indicating VNp is not required to maintain solubility once expressed.

To explore whether dimerisation was sufficient to induce internalisation of a VNp-fusion protein, stable alpha-helical VNp-dimers were created by introducing a leucine-zipper (LZ) sequence [9] between VNp and cargo (Fig. 3, Supplementary Fig. 3). Expression of the VNp-LZ fusion induced formation of cytosolic VNp-LZ-fusion filled vesicular structures, which form from the CydAB [10] containing inner-membrane (Fig. 3b-d; Supplementary Video 1). While the precise molecular basis is not yet understood, these data illustrate dimerised VNp-fusions promote inward rather than outward curvature of the bacterial membrane, to provide an attractive method for generating recombinant proteins within cytosolic membrane bound structures to further facilitate the production of disulphide bond containing and otherwise insoluble or toxic proteins from *E. coli*.

Spurred on by the success of this approach, we asked whether simple modifications to the VNp amino acid sequence to modulate the ability to form VNp-fusion containing vesicles would enhance the exported protein yields. We therefore systematically tested equivalent VNp sequences from the β- and γ-synuclein isoforms (Table 1) as well as a series of constructs generated through modifying charges and side chain length of targeted residues along the helix surface found that we could not only enhance vesicular export over a wide range of culture temperatures (VNp6), but also reduce the size of the VNp to 20 residues length (VNp15) to enhance the export of the target model biopharmaceuticals DARP and Stefin-A at yields of more than 2.5 g of soluble recombinant protein / litre of bacterial flask culture (Table 1). These high yields were reproducible in both academic and industrial environments.

The VNp system exhibits flexibility as vesicle packaged proteins can be generated in different *E. coli* strains (e.g BL21, λ, JM109 and K12 lineages. Supplementary Fig. 4,) making it perfectly suited for the production of synthetic proteins with modifications supported by specialist *E. coli* hosts. For example, the VNp system functions in W3110 cells, which allows generation of recombinant protein filled vesicles with a reduced immunogenic response [11]. VNp-fusions can be expressed from a variety of plasmids (including pUC19 and pBR322 based derivatives) and modulated VNp-fusion expression can be driven from diverse promoters (e.g. T7, rhamnose) and induction levels (Supplementary Fig. 4, Table 1), making this a truly versatile system.

Unlike native outer membrane vesicles that occur naturally in *E. coli*, which form spontaneously in the absence of recombinant protein expression [12-14], the VNp system described here nucleates vesicle formation through interactions with the inner membrane. In addition while recombinant proteins are absent from native vesicles released into the media when expressed *E. coli* cells, the VNp system allows a simple tagging mechanism for targeted recombinant proteins into vesicles (Table 1). This simple peptide fusion increases yields and simplifies downstream processing of a wide range of recombinant proteins from *E. coli*. Importantly, the ease with which otherwise insoluble or toxic proteins can be isolated in milligram or gram quantities suggests that this approach is an attractive starting point for the expression of any recombinant protein of interest. It should be noted that the isolation of protein from VNp-fusion induced vesicles is unlikely to provide a route to avoid endotoxin entirely, as proteins

are always wrapped in endotoxin during normal secretion processes or homogenisations. Therefore, depending upon the downstream application, the enriched - VNp derived proteins may require further purification. The method has the potential to allow continuous release of protein from extended period cultures in appropriately genetically modified stable expression strains. Another beneficial aspect of this innovation is the stability of proteins and preservation of enzymatic activity when the vesicles are maintained at 4 ºC. As the use of this system is more broadly adopted and further enhancements and adaptations emerge, its impact can be anticipated to be highly significant. We therefore predict rapid adoption of this versatile system into a wide range of downstream processes and applications.

LIMITATIONS OF STUDY

While there is no guarantee this system will enhance production for all proteins, its use resulted in significant increase in yield and solubility for each of the proteins we have tested to date (n>60). While some of the recombinant protein filled vesicles remain cytosolic, it is our experience that these tend to be either dimeric, disulphide bond containing or toxic proteins, which may reflect differences in localised membrane conformation and/or membrane affinity. However in each of these cases we also observed enhanced expression and / or functionality of the subsequently expressed proteins. The model depicted in Figure 1j represents a model of how the system works, based on current biochemical and imaging data presented in this study. Elucidating the membrane composition of the vesicles and further *in vitro* studies will provide insight into the precise mechanism underlying the formation of the recombinant protein filled vesicles, described here.

ACKNOWLEDGEMENTS

The authors thank J. Walklate for assistance undertaking stopped-flow experiments, S. Boxall, M. Geeves, I. Hagan, and D. Manstein for stimulating discussions and comments on the manuscript. This work was supported by the University of Kent and funding from the Biotechnology and Biological Sciences Research Council (BB/S005544/1 & BB/L013703/1_D0101) and Fujifilm-Diosynth Biotechnologies UK Ltd.

AUTHOR CONTRIBUTIONS

TAE, KB, BRS and NA performed the experimental studies; LW supervised Structured Illumination Microscopy; SWB supervised Fluorescence Lifetime Microscopy; IRB undertook Transmission Electron Microscopy; JRH supervised lipid binding studies; CL undertook fermentation experiments; TAE, KB, CL and DPM designed experiments; DPM sought funding and supervised the project. DPM wrote the main drafts of the manuscript and all authors contributed to editing.

FIGURE LEGENDS

Figure 1 *Recombinant vesicle formation*. (a) SIM fluorescence images of E.coli expressing αSyn-mNeongreen (green) and OmpA-mCherry (red) show production of extracellular αSyn containing membrane vesicles. (b) OmpA-mCherry SIM fluorescence and (c & d) TEM images illustrating VNp induced membrane curvature in *E. coli*. (e) EM of vesicles generated from VNp expressing *E. coli* cells that were cultured on prepared grids. (f) mCherry (magenta) and mNeongreen (green) SIM fluorescence of VNp-mNeongreen OmpA-mCherry expressing *E. coli* cells. (g) Anti-mNeongreen immuno-EM of a section though *E. coli* associated VNp-mNeongreen induced vesicle. (h) TEM images of isolated VNp-mNeongreen containing vesicles. (i) Coomassie stained gel of cell culture and filtered media of VNp-mNeongreen expressing cells. (j) Schematic of VNp induced cargo containing vesicles. (k) Coomassie stained samples of uninduced and induced cultures or filtered induced cultures of VNp-DARP, VNp-Uricase and VNp-StefinA expressing cells. (l & m) Average soluble yields per litre of culture derived from cell extracts (empty boxes) or filtered culture media (filled boxes) for each recombinant protein examined. Recombinant proteins lacked (l) or possessed (m) a fluorescent mNeongreen fusion. Errors are s.d. from ≥ 3 experimental repeats.

Figure 2 *VNp allows expression of functional disulphide bond containing IgG1 fusion dimers.* (a) conventionally stained and (b) anti-mNeongreen immuno-stained EM serial section images of VNp-mNeongreen-Etanercerpt induced inward membrane curvature in *E. coli*. (c) Schematic of the VNp-mNeongreen-TEV-Etanercept fusion protein. (d & e) Anti-mNeongreen western blots illustrating disulphide bond dependent oligomerisation (d) and protein A binding IgG1 functionality (e) of VNp-mNG-Etanercept purified from *E. coli*. (d) VNp-mNG-Etanercept disulphide bond-dependent oligomers (*) are disrupted by the addition of the disulphide bond disrupting reducing agent, DTT. (e) VNp-mNG-Etanercept-His_6 fusion was affinity purified from *E. coli* and bound to Protein A – Dynabeads. Beads were subsequently washed in binding buffer, before being boiled in SDS-PAGE loading buffer to release bound proteins. Predicted size of VNp-mNeongreen-Etanercept: 83.9 kDa. (f) Anti-His western blot of wash (unbound) and Protein A bound fractions of TEV cleaved VNp-mNeongreen-TEV-

Etanercept-His fusion mixed with Protein A-Dynabeads. Predicted size of Etanercept: 52.5 kDa. This illustrates unlabelled Etanercept remains soluble and functional upon removal of the VNp-mNeongreen tag.

Figure 3 *VNp dimers produce VNp-fusion containing cellular membrane packages.* (a) Size exclusion chromatography profiles of purified recombinant VNp-mNG and VNp-LZ-mNG proteins (inset) confirmed introduction of a Leucine Zipper (LZ) motif to the VNp-mNeongreen (mNG) fusion induced stable dimer formation. Each fusion protein as well protein standards (29 kDa carbonic anhydrase - blue; 66 kDa BSA – red; 443 kDa Apoferritin complex - yellow), were run using identical conditions. While the VNp-mNG (black) elution profile was consistent with a monomeric protein, the VNp-LZ-mNG (grey) eluted from the column in earlier fractions consistent with it existing predominantly as a dimer. (b & c) Anti-mNeongreen immuno-EM images of sections though *E. coli* expressing VNp-LZ-mNeongreen, and (d) SIM images of CydAB-mNeongreen labelled inner membranes in *E. coli* expressing VNp-LZ show the VNp-LZ dimer concentrates within the lumen of cytosolic inner membrane bound vesicles.

TABLE AND LEGEND

Protein	Total yield	Cytosolic	Exported	% Export
mNeongreen	59	59 ± 10	n.d.	0
DARP	32	32 ± 11	n.d.	0
Uricase	402	402±101	n.d.	0
StefinA	374	374 ± 15	n.d.	0
EPO	0	n.d.	n.d.	0
FGF21	0	n.d.	n.d.	0
Etanercept	0	n.d.	n.d.	0
hGH	0	n.d.	n.d.	0
VNp-mNeongreen	472	55 ± 4	417 ± 0	88
VNp-DARP	941	76 ± 44	865 ± 12	92
VNp-Uricase	900	577 ± 146	323 ± 123	36
VNp-StefinA	505	99 ± 6	406 ± 123	80
VNp-FGF21	52	n.d.	52 ± 6	100
VNp-EPO	0	n.d.	n.d.	0
VNp-Etanercept (*10 µg/ml IPTG*)	0	n.d.	n.d.	0
VNp-hGH (*10 µg/ml IPTG*)	0	n.d.	n.d.	0
mNG-DARP	128	128 ± 21	n.d.	0
mNG-Uricase	33	33 ± 2	n.d.	0
mNG-StefinA	12	12 ± 1	n.d.	0
mNG-EPO	15	15 ± 2	n.d.	0
mNG-FGF21	9	9 ± 1	n.d.	0
mNG-Etanercept (*10 µg/ml IPTG*)	14	14 ± 3	n.d.	0
mNG-hGH (*10 µg/ml IPTG*)	16	16 ± 3	n.d.	0
VNp-mNG-DARP	701	164 ± 45	537 ± 28	77
VNp-mNG-Uricase	212	103 ± 16	110 ± 29	52
VNp-mNG-StefinA	172	70 ± 24	102 ± 32	59
VNp-mNG-EPO	32	13 ± 2	19 ± 6	61
VNp-mNG-anti-GFP_nanobody	194	194 ± 5	0	0
VNp-mNG-FGF21	23	10 ± 1	13 ± 5	57
VNp-mNG-Etanercept (*10 µg/ml IPTG*)	177	170 ± 22	7 ± 5	4
VNp-mNG-hGH (10 µg/ml IPTG)	60	58 ± 8.5	3 ±1	4
VNp-LZ-mNeongreen	393	56 ± 29	337 ± 17	86
VNp-LZ-hGH	10	n.d.	10 ± 2	100
VNp-mNeongreen (*50 µg/ml IPTG*)	411	167 ± 114	241 ± 24	59
VNp-mNeongreen (*100 µg/ml IPTG*)	287	59 ± 35	227 ± 28	79

VNp (β-isoform) -mNeongreen	390	284 ± 73	106 ± 15	27
VNp (γ-isoform) -mNeongreen	682	252 ± 159	429 ± 155	63
VNp6-mNeongreen	639	53 ± 22	586 ± 15	92
VNp15-mNeongreen	697	76 ± 20	621 ± 38	89
VNp6-DARP	2,194	50 ± 34	2145 ± 126	97.7
VNp15-DARP	1,632	104 ± 28	1528 ± 55	93.6
VNp6-StefinA	1,884	43 ± 14	1841 ± 132	97.7
VNp15-StefinA	2,584	320 ± 34	2264 ± 153	87.6
VNp-mNeongreen (*30 ºC*)	490	314 ± 46	176 ± 28	36
VNp6-mNeongreen (*30 ºC*)	554	111 ± 25	443 ± 13	80
VNp-mNeongreen (*25 ºC*)	358	241 ± 0	117 ± 9	33
VNp6-mNeongreen (*25 ºC*)	520	334 ± 10	187 ± 2	36

Table 1 *Summary of soluble protein yields from shaking flask cultures.* Yields measured as mg of soluble recombinant protein / litre. Cells grown in shaking flask cultures at 37 ºC with T7 promoter induced with 20 µg / ml IPTG unless stated otherwise. All cultures had reached stationary phase with undiluted OD_{600} of ~2 (i.e. equivalent cell densities) at the time of harvesting. Average yields ± s.d. calculated from ≥ 3 independent biological repeats. n.d.: not detectable.

STAR METHODS

Resource Availability

Lead contact

Further information and requests for resources and reagents should be directed to and will be fulfilled upon reasonable request by the Lead Contact Dan Mulvihill (d.p.mulvihill@kent.ac.uk)

Materials availability

Plasmids generated in this study have been deposited to Addgene. Plasmid ID #s 182386 – 182425.

Data and code availability

- All the Raw datasets generated during this study have been deposited at Kent Data Repository and are publicly available as of the date of publication. Microscopy data reported in this study will be shared by the lead contact upon request.
- This paper does not report original code.
- Any additional information required to reanalyze the data reported in this paper is available from the lead contact upon request.

Experimental model and subject details

E. coli strains used in this study:

BL21 DE3 F$^-$*omp*T *hsd*S$_B$ (r_B^-, m_B^-) *gal dcm* (DE3).
DH10b F$^-$*mcr*A Δ(*mrr-hsd*RMS-*mcr*BC) φ80*lac*ZΔM15 Δ*lac*X74 *rec*A1 *end*A1 *ara*D139 Δ(*ara-leu*)7697 *gal*U *gal*K λ$^-$*rps*L(Str^R) *nup*G
W3110 F$^-$ *λ*$^-$ *IN(rrnD-rrnE)1 rph-1*
CLD1040 F$^-$ *λ*, *IN(rrnD-rrnE)1 rph-1 OmpT*
JM109 F$^-$ *tra*D36 *pro*AB *laq*I^{q}ZΔM15 *end*A1 *rec*A1 *gyr*A96 *thi hsd*R17 (r_k^-, m_k^+) *rel*A1 *sup*E44 Δ (*lac-pro*AB)

Bacterial cell Culture and protein induction - All bacterial cells were cultured at 37 ºC using LB (10 g Tryptone; 10g NaCl; 5g Yeast Extract (per litre)) and TB (12g Tryptone; 24g Yeast Extract; 4ml 10% glycerol; 17 mM KH_2PO4 72 mM K_2HPO_4 (per litre) media. 5 ml LB starters from fresh bacterial transformations were cultured at 37 ºC to saturation and used to inoculate 100 - 500 ml volume TB media, flask cultures that were incubated overnight at 37 ºC with 200 rpm orbital shaking. Recombinant protein expression from the T7 promoter was induced by addition of IPTG to a final concentration of 20 µg / ml (except etanercept where 10 µg / ml was

used) once the culture had reached an OD_{600} of 0.8 – 1.0). Growth curves were generated from 96 well plate cultures, prepared from late log-phase cultures, diluted into fresh media to an OD_{600} of 0.1 nm at the start of the growth analysis experiment. OD_{600} absorbance values were obtained using a Thermo Scientific Multiscan Go 1510-0318C plate reader and recorded using the SkanIt Software 4.0. at OD_{600} values were taken every 15 minutes for the duration of the experiment, and growth curves generated from averages of 4 individual biological repeats.

Method details

Soluble protein extracts - cell pellets from 50 ml of culture were resuspended in 5 ml of soluble extract buffer (20 mM TRIS, 500 mM NaCl, pH 8.0), sonicated for a total of 2 min (6 x 20 sec pulses), and cell debris removed by centrifugation at 18,000 rpm (4 ºC) for 30 min. Target protein concentration was determined using fluorescence of mNeonGreen fusion or gel densitometry. Both techniques were compared directly on the same samples to determine equivalence.

Recombinant vesicle isolation: Vesicles were isolated directly from bacterial cell cultures by passing the culture through a 0.45 µm PES filter. Typical purity and concentration from equivalent volume of culture and filter flow through are shown in Fig. 1. Exclusion of viable cells from the vesicle containing filtrate was routinely tested by plating onto LB plates lacking antibiotics and incubating overnight at 37 ºC (example shown in Supplemental Figure 2)

Protein concentration determination: Fluorescence scan was used to determine concentration of mNeongreen fusion proteins in vesicle containing media and soluble protein extracts. Absorbance was measured at 506 nm using a Varian Cary 50 Bio UV-Vis spectrophotometer, with measurements from an equivalent empty vector culture used for baseline correction, and concentration determined using an extinction coefficient of 116,000 $M^{-1}cm^{-1}$. Concentration of non-mNeongreen labelled proteins was determined by gel densitometry analysis of triplicate samples run alongside BSA loading standards on Coomassie stained SDS-PAGE gels. Gels were scanned and analysed using Image J software. Concentration was determined by both UV and densitometry for three independent VNp-mNeongreen samples to confirm parity between techniques. Average yields in Fig1 & Table S1 were calculated (mg target protein / litre culture) from a minimum of 3 independent biological repeats from cultures of BL21 DE3 *E. coli* cells grown in TB media.

Protein isolation from vesicles: Purified VNp induced vesicles were resuspended in ice cold 1xPBS before being sonicated to disrupt vesicle membrane, and release the VNp-fusion protein. In order to further purify carboxyl His_6 tagged recombinant VNp-fusion protein (all recombinant proteins expressed during this study contain carboxyl-terminal His_6 affinity tags),

this solution was then mixed in a 1 in 5 dilution of 5 x binding buffer (250 mM TRIS 2.5 M NaCl 5% Triton-X 50 mM Imidazole pH 7.8) before passing over a Ni^{2+}-agarose resin gravity column. Cytosolic recombinant protein was purified by passing soluble protein extracts (supplemented with Imidazole to 20 mM) over the Ni^{2+}-agarose resin gravity column. In both cases matrix bound His-tagged protein was washed, eluted (using imidazole), and dialysed into appropriate storage or assay buffer. Protein identity and amino-terminal acetylation of isolated proteins was confirmed by electrospray mass-spectroscopy.

Circular Dichroism (CD): Measurements were made in 2 mm quartz cuvettes using a Jasco 715 spectropolarimeter. VNp protein and 100 nm extruded vesicles were diluted in CD buffer (10 mM potassium phosphate, 5 mM $MgCl_2$ pH 7.0) to a concentration of 0.4 mg/ml and 0.2 respectively. Broad negative peaks at 208 and 222 nm and a positive peak at < 200 nm are consistent with an α-helical structure.

Electrospray LC-MS of Proteins: Electrospray mass spectra were recorded on a Bruker micrOTOF-Q II mass spectrometer. Samples were desalted on-line by reverse-phase HPLC on a Phenomenex Jupiter C4 column (5 µm, 300 Å, 2.0 mm x 50 mm) running on an Agilent 1100 HPLC system at a flow rate of 0.2 ml/min using a short water, acetonitrile, 0.05% trifluoroacetic acid gradient. The eluant was monitored at 214 nm & 280 nm and then directed into the electrospray source, operating in positive ion mode, at 4.5 kV and mass spectra recorded from 500-3000 m/z. Data was analysed and deconvoluted to give uncharged protein masses with Bruker's Compass Data Analysis software.

In-gel tryptic digest and proteomic analysis of recombinant vesicles: Sample of purified VNp-DARP induced vesicles (shown in Fig S5b) were run on SDS-PAGE, which was subsequently coomassie stained, and the whole sample lane cut out, cut into small pieces, which were subsequently transferred to a 1.5 ml microfuge tube and stored in distilled water at 4 ºC until processing. The gel particles were washed with 150 µl of freshly made 50 mM NH_4HCO_3: acetonitrile (1:1 ratio) for 15 mins. Liquid was removed and gel fragments resuspended in 150 µl acetonitrile for 15 mins, before liquid was again removed, and gel pieces were resuspended in 100 ml of 10 mM DTT in 50 mM NH_4HCO_3, and incubated for 30 min. at 56 °C. Gel pieces were centrifuged, and excess liquid removed before incubating for 1 min with 100 µl of acetonitrile, which was again removed and gel fragments were suspended in 100 ml of 55 mM chloroacetamide in 50 mM NH_4HCO_3 and incubated for 20 min at room temp in the dark. Pellets were then centrifuged, the chloroacetamide solution was removed. Gel pieces were subject to subsequent 15 min washes in 150 ml of 50 mM NH_4HCO_3:acetonitrile (1:1), and then150 ml of 50 mM NH_4HCO_3 for 15 min, and liquid was removed by centrifugation after each wash. Gel pieces were then washed for 15 mins with 200 µl of acetonitrile, and then rehydrated in 50 ml of digestion buffer (12.5 mM NH_4HCO_3,

10% acetonitrile) containing 5 ng/ml of trypsin, which was left overnight at room temperature. Upon completion of digestion, 15 ml acetonitrile was added to the sample, where was then sonicate in an ultrasound bath for 15 mins. Gel fragments were isolated by centrifugation and the supernatant collected in a fresh 0.5 ml microfuge tube (A). The gel fragment pellet was resuspended in 30 µl 50% acetonitrile with 5% formic acid, and sonicate in an ultrasound bath for 15 mins, and pellet again isolated by centrifugation and supernatant collected in a fresh 0.5 ml microfuge tube (B). Contents of tube A and B were combined, vacuum dried, and subsequently resuspended in 20 ml of 5% acetonitrile, 0.1% TFA. Samples were run through Pierce C18 Spin Tips and analysis by nano-LCMS.

Gel filtration assay: 500 µl of protein samples were loaded to a Superdex 200 Increase 10/300 GL size-exclusion column (GE Healthcare Life Sciences) equilibrated at room temperature in PBS and run at 0.75 ml/min flow rate. Eluted proteins were measured by Viscotek Sec-Mals 9 and Viscotek RI detector VE3580 (Malvern Panalytical).

Lipid binding Assay: Affinity of VNp for *E. coli* membrane lipids was established using a thermal shift fluorescence binding assay adapted from [15]. Equivalent assay samples, made up of: 65 µl 3 mg/ml of VNp-mNeongreen, 65 µl 1 mM of 100 nm extruded vesicles composed of the lipid mixture to be tested; 15 µl, 10%OGP; and 5 µl 20 mM Tris-HCl pH 7.0, were prepared in PCR tubes and held at the defined temperature in a gradient PCR machine for 10 minutes. Samples were centrifuged at 18,000 *xg*, and supernatant fluorescence was determined in black 96 well plates (BRAND, Germany) using a BMG Clariostar (BMG Labtech). Fluorescence readings were normalised and used to create a melting curve, where the melting temperature (*Tm*) was determined using Origin software (OriginLab). The final *Tm* value was an average (± s.d) calculated from three independent sample repeats.

Uricase Assay: 500 µl of 100 mM Tris pH 8.5 with 200 mM Uric acid was placed in a cuvette and OD_{293} measurements were taken over for 4 or 5 minutes. Subsequently either 500 µl of 4.5 mg/ml purified VNp2-Uricase (dialysed into 0.1 M Tris pH 8.5) or dialysis buffer alone was added to the cuvette and OD_{293} measurements taken for 25 mins. (Adapted from [16]).

Widefield Fluorescence Microscopy: Cells were mounted onto coverslips under < 1 mm thick circular LB-agarose(2%) pads, and attached with appropriate spacers onto glass slides, before being visualised on an inverted microscope [17]. All live cell imaging for each sample was completed within 30 mins of mounting cells onto coverslips.

Structured Illumination Microscopy (SIM) was undertaken using a Zeiss Elyra PS 1 microscope with a 100x NA 1.46 oil immersion objective lens (Zeiss α Plan-Apochromat) as described previously. [18,19] Briefly, cells were mounted under thin LB-agarose pads onto high precision No.1.5 coverslips (Zeiss, Jenna, Germany). 488 nm and 561 nm laser were used to

illuminate mNeongreen and mCherry/mScarlet fusions, respectively. The optical filter set consisted of laser blocking filter MBS 405/488/561 as the dichroic mirror, and the dual-band emission filter LBF-488/561. The total of 3 rotations of the illumination pattern were implemented to obtain two-dimensional information. Super-resolution SIM image processing was performed using the Zeiss Zen software. Two colour images were aligned using the same software following a calibration using pre-mounted MultiSpec bead sample.

Fluorescence Lifetime Imaging Microscopy (FLIM): The one- and two- photon systems used in this work have been previously described. [20]. Prior to FLIM data acquisition, protein expression levels were verified using confocal microscope. Here, a Nikon Eclipse C2-Si confocal scan head attached to an inverted Nikon TE2000 or Ti-E microscope was used. mNeongreen and mCherry FP were excited at 491 nm (emission 520/35 nm) and 561 nm (emission 630/50 nm) respectively using an NKT super continuum laser. FLIM images were obtained as follows: 2 photon (950 nm) wavelength light was generated by a mode-locked titanium sapphire laser (Mira F900, Coherent Laser Ltd), producing 180 fs pulses at 76 MHz. This laser was pumped by a solid-state continuous wave 532 nm laser (Verdi 18, Coherent Lasers Ltd). Fluorescence was collected through a BG39 filter for the donor fluorophore. The acceptor was not excited.

For one photon excitation FLIM, the system is equipped with a SuperK EXTREME NKT-SC 470-2000 nm supercontinuum laser (NKT Photonics) which generates at 80 MHz repetition rate with 70 ps pulse width. The desired wavelengths were selected using a SuperK SELECT 29 multi-line tunable filter (NKT photonics). Images were collected through either a 60X 1.2 NA water immersion (Fig. S1c&d) or 60X 1.49 NA oil immersion (Fig. S1e) lens. For both one and two-photon excitation, emission was collected by the same objective through filters (above) and detected with an external hybrid GaAsP (HPM-100-40, Becker & Hickl, Germany), linked to a time correlated single photon counting (TCSPC) module (SPC830, Becker and Hickl, Germany). Photon counts of at least 1000 used for the multi-exponential analysis. Raw time correlated single photon counting decay curve at each pixel (256 x 256 or higher) of the images were analysed using SPCImage software v.6.9 (Becker and Hickl, GmbH); an incomplete single exponential fit model with a laser repetition time value of 12.5 ns was used for the decay curve fitting. Lifetime values with $\chi 2$ between 0.8 and 1.3 were taken as a good exponential decay fit.

TEM analysis of cells and isolated vesicles: Negative stained TEM samples of cells and vesicles were prepared in one of two ways.10 µl of *E. coli* cells expressing VNp-mNeongreen from an overnight culture was placed onto a formvar/carbon coated 400mesh gold grid and incubated in a humid chamber at 37 ºC to allow vesicle formation. Recombinant vesicles isolated from a culture of *E. coli* expressing VNp-mNeongreen were placed onto a

formvar/carbon coated 600mesh copper grid and left for 5 mins at room temperature to allow vesicles to settle onto the surface. Both samples were then fixed in 2.5% glutaraldehyde in 100 mM sodium cacodylate buffer pH 7.2 (CAB) for 10 minutes. Grids were then washed in 100 mM CAB and milliQ water. Grids were then dried and negative stained for 5 seconds in 2% aqueous uranyl acetate.

TEM thin section analysis of *E. coli* cells: *E. coli* expressing VNp-mNeongreen were cultured as described above and harvested by centrifugation at 3,000 *g* for 10 min. The cell pellet (approximately 100µl) was resuspended in 2 ml of 2.5% (w/v) glutaraldehyde in CAB and fixed for 2 hr at RT with gentle rotating (20 rpm). Cells were pelleted by centrifugation at 6,000 *g* for 2 min and were washed twice for 10 min with 100 mM CAB. Cells were postfixed with 1% (w/v) osmium tetroxide in 100 mM CAB for 2 hr and subsequently washed twice with ddH2O. Cells were dehydrated by incubation in an ethanol gradient, 50% EtOH for 10 min, 70% EtOH overnight, and 90% EtOH for 10 min followed by three 10-min washes in 100% dry EtOH. Cells were then washed twice with propylene oxide for 15 min. Cell pellets were embedded by re- suspension in 1 ml of a 1:1 mix of propylene oxide and Agar LV Resin and incubated for 30 min with rotation. Cell pellets were infiltrated twice in 100% Agar LV resin (2 x 2h). The cell pellet was resuspended in fresh resin and transferred to a 1-mL BEEM embedding capsule, centrifuged for 5 min at 1100 rpm in a swing out rotor to concentrate the cells in the tip of the capsule and samples were polymerised for 20 hr at 60°C.

Ultrathin sections were cut using a Leica EM UC7 ultramicrotome equipped with a diamond knife (DiATOME 45°). Sections (70 nm) were collected on uncoated 400-mesh copper grids. Grids were stained by incubation in 4.5% (w/v) uranyl acetate in 1% (v/v) acetic acid for 45 min followed by washing in a stream of ddH2O. Grids were then stained with Reynolds lead citrate for 7 min followed by washing in a stream of ddH2O. Electron microscopy was performed using a JEOL-1230 transmission electron microscope operated at an accelerating voltage of 80 kV equipped with a Gatan One View digital camera.

Immuno-EM of isolated vesicles: 2µl of filtered media containing recombinant vesicles from a culture of *E. coli* expressing VNp-mNeongreen was placed onto a formvar/carbon coated 600 mesh copper grid and left for 5 mins at room temperature to allow vesicles to settle. Vesicles were osmotically shocked to rupture vesicles by moving grids into 2 x 20µl drops of milliQ water for 10 minutes at RT. Samples were then fixed in 2% formaldehyde and 0.5% glutaraldehyde in CAB for 15 minutes at RT. Grids were then washed in 6 x 20µl drops of CAB and 6 x 20µl drops of TBST (20 mM Tris-HCl, 500 mM NaCl, 0.05% Tween 20 and 0.1% BSA pH7.4). Samples were blocked in a 20µl drop of 2% BSA in TBST at room temperature for 30 min. Grids were then transferred directly into a 20µl drop of anti-mNeongreen rabbit polyclonal (Cell Signalling Technology) primary antibody diluted 1:100 in TBST and incubated for 1 hr.

Grids were washed in 6 x 20µl drops of TBST. Grids were then moved into a drop of goat anti-rabbit IgG 5nm gold (British Biocell International) diluted 1:50 and then moved to a fresh drop of the same antibody and incubated for 30 min. Excess antibody was removed by washing in 6 x 20µl drops of TBST and 6 x 20µl drops of milliQ water and dried.

Grids were negative stained for 5 seconds in 2% aqueous uranyl acetate. Electron microscopy was performed using a JEOL-1230 transmission electron microscope operated at an accelerating voltage of 80 kV equipped with a Gatan One View digital camera.

Immuno-EM of *E. coli* cells: *E. coli* expressing VNp-mNeongreen were cultured as described above and harvested by centrifugation at 3,000 *g* for 10 min. The cell pellet (approximately 100µl) was resuspended in 2 ml 2% (w/v) formaldehyde and 0.5% glutaraldehyde in CAB and fixed for 2h at RT. The sample was washed 2 x10 minutes in CAB. Cells were dehydrated by incubation in an ethanol gradient, 50% EtOH for 10 min, 70% EtOH overnight, and 90% EtOH for 10 min followed by three 10-min washes in 100% dry EtOH. Cells were then suspended in LR White resin medium grade (London Resin Company) for 4h and then in fresh LR White resin overnight. Following 2 x 4h changes in fresh LR White resin samples were placed in sealed gelatine capsules and spun in a swing out rotor at 1100rpm to concentrate cells. Gelatine capsules containing the cell pellets were polymerised upright at 60ºC for 20 hours. Ultrathin sections were cut using a Leica EM UC7 ultramicrotome equipped with a diamond knife (DiATOME 45°). Sections (80 nm) were collected on uncoated 400-mesh gold grids.

Samples were blocked in a 20µl drop of 2% BSA in TBST at room temperature for 30 min. Grids were then transferred directly into a 20µl drop of anti-mNeongreen rabbit polyclonal (Cell Signalling Technology) primary antibody diluted 1:10 in TBST and incubated for 1 hr. Grids were washed in 6 x TBST. Grids were then moved into a drop of goat anti-rabbit IgG 5nm gold (British Biocell International) diluted 1:50 and then moved to a fresh drop of the same antibody and incubated for 30 min. Excess antibody was removed by washing in 6 x 20µl drops of TBST and 6 x 20µl drops of milliQ water and dried.

Grids were stained for 15 min in 4.5% uranyl acetate in 1% acetic acid solution and then washed in 6 x 20µl drops of milliQ water. Grids were then stained with Reynolds lead citrate for 3 min and washed in 6 x 20µl drops of milliQ water. Electron microscopy was performed using a JEOL-1230 transmission electron microscope operated at an accelerating voltage of 80 kV equipped with a Gatan One View digital camera.

Quantification and Statistical Analysis: Statistical details of experiments can be found in the figure legends, including a definition of exact values of n, and details of error bars.

DECLARATION OF INTERESTS

CL is an employee at Fujifilm-Diosynth Biotechnologies UK Ltd. The remaining authors declare no competing interests. The Vesicle Nucleating peptide technology described here is associated with patent application # *GB2118435.3*.

REFERENCES

1. Kim, J.H., Lee, J., Park, J., Gho, Y.S. (2015). Gram-negative and Gram-positive bacterial extracellular vesicles. *Semin Cell Dev Biol*, 40, 97-104.

2. Eastwood, T.A., Baker, K., Brooker, H.R., Frank, S., Mulvihill, D.P. (2017). An enhanced recombinant amino-terminal acetylation system and novel in vivo high-throughput screen for molecules affecting α-synuclein oligomerisation. *FEBS Letters*, 106, 8157-8159.

3. Bartels, T., Kim, N.C., Luth, E.S., Selkoe, D.J. (2014). N-alpha-acetylation of α-synuclein increases its helical folding propensity, GM1 binding specificity and resistance to aggregation. *PLoS ONE*, 9(7), e103727.

4. Fusco, G., Pape, T., Stephens, A.D., et al. (2016). Structural basis of synaptic vesicle assembly promoted by alpha-synuclein. *Nat Commun*, 7(1), 1-11.

5. Shaner, N.C., Lambert, G.G., Chammas, A., et al. (2013). A bright monomeric green fluorescent protein derived from Branchiostoma lanceolatum. *Nat Meth*, 10(5), 407-409.

6. Kodama, Y., Hu, C.D. (2010). An improved bimolecular fluorescence complementation assay with a high signal-to-noise ratio. *BioTechniques*, 49(5), 793-805.

7. Goffe, B., Cather, J.C. (2003). Etanercept: An overview. *J Am Acad Dermatol*, 49(2), S105-S111.

8. Ultsch, M.H., Somers, W. (1994). The crystal structure of affinity-matured human growth hormone at 2 Å resolution. *J Mol Biol*, 236, 286-299.

9. O'Shea, E.K., Klemm, J.D., Kim, P.S., Alber, T. (1991). X-ray structure of the GCN4 leucine zipper, a two-stranded, parallel coiled coil. *Science*, 254(5031), 539-544.

10. Safarian, S., Rajendran, C., Mueller, H., et al. (2016). Structure of a bd oxidase indicates similar mechanisms for membrane-integrated oxygen reductases. *Science*, 352(6285), 583-586.

11. Gujrati, V., Prakash, J., Malekzadeh-Najafabadi, J., et al. (2019). Bioengineered bacterial vesicles as biological nano-heaters for optoacoustic imaging. *Nat Commun*, 10(1), 1114.

12. Blackburn, S.A., Shepherd, M., Robinson, G.K. (2021). Reciprocal Packaging of the Main Structural Proteins of Type 1 Fimbriae and Flagella in the Outer Membrane Vesicles of “Wild Type” Escherichia coli Strains. *Front Microbiol*, 12, 557455.

13. Hong, J., Dauros-Singorenko, P., Whitcombe, A., et al. (2019). Analysis of the Escherichia coli extracellular vesicle proteome identifies markers of purity and culture conditions. *J Extracell Vesicles*, 8(1),1632099.

14. Thoma, J., Manioglu, S., Kalbermatter, D., Bosshart, P.D., Fotiadis, D., Muller, D.J. (2018). Protein-enriched outer membrane vesicles as a native platform for outer membrane protein studies. *Commun Biol*, 1, 23.

15. Nji, E., Chatzikyriakidou, Y., Landreh, M., Drew, D. (2018). An engineered thermal-shift screen reveals specific lipid preferences of eukaryotic and prokaryotic membrane proteins. *Nat Commun*, 9(1), 4253–12.

16. Huang, S.H., Wu, T.K. (2004). Modified colorimetric assay for uricase activity and a screen for mutant Bacillus subtilis uricase genes following StEP mutagenesis. *Eur J Biochem*, 271(3), 517-523.

17. Mulvihill, D.P. (2017). Live cell imaging in fission yeast. *Cold Spring Harb Protoc*. (10), 761-773.

18. Periz, J., Rosario, M., McStea, A., et al. (2019). A highly dynamic F-actin network regulates transport and recycling of micronemes in Toxoplasma gondii vacuoles. *Nat Commun*. September:1-16.

19. Qiu, H., Gao, Y., Boott, C.E., et al. (2016). Uniform patchy and hollow rectangular platelet micelles from crystallizable polymer blends. *Science*. 352(6286), 697-701.

20. Botchway, S.W., Scherer, K.M., Hook, S., et al. (2015). A series of flexible design adaptations to the Nikon E-C1 and E-C2 confocal microscope systems for UV, multiphoton and FLIM imaging. *J Microsc*. 258(1), 68-78.

Key Resource Table

KEY RESOURCES TABLE

REAGENT or RESOURCE	SOURCE	IDENTIFIER
Antibodies		
Rabbit anti-mNeonGreen tag	Cell Signaling Technology	Cat#53061
Mouse anti 6x His	Invitrogen	Cat#15287848
Bacterial and virus strains		
BL21 DE3 (DE3)	Lab stock	
DH10b	Lab stock	
W3110	Lab stock	
CLD1040	Lab stock	
JM109	Lab stock	
Deposited data		
Raw and analysed data	This study: Kent Data Repository	DOI: 10.22024/UniKent/01.01.416.
VNp and LZ peptide sequences		
VNp	MDVFMKGLSKAKEGVVAAAEKTKQGVAEAAGKTKEGVL	
VNp6	MDVFKKGFSIADEGVVGAVEKTDQGVTEAAEKTKEGVM	
VNp15	MDVFKKGFSIADEGVVGAVE	
Uniprot accession numbers of protein cargoes tested in this study		
DARP	Designed Ankyrin Repeat Protein off7 (*Agrobacterium radiobacter*)	B9JMD9
DNase	Deoxyribonuclease I (*Bos taurus*)	P00639
EPO	Erythropoietin (*Homo sapiens*)	P01588
Etanercept	Tumour necrosis factor receptor 1B - IgG1 fusion (*Homo sapiens*)	P20333
FGF21	Fibroblast Growth Factor 21 (*Homo sapiens*)	Q9NSA1
hGH	Somatotrophin (*Homo sapiens*)	P01241
mNeongreen	mNeongreen (*Branchiostoma lanceolatum*)	A0A1S4NYF2
StefinA	Cystatin-A (*Homo sapiens*)	P01040
Uricase	Uricase (*Cyberlindnera jadinii*)	P78609
Recombinant DNA		
pRSFDuet-1_VNp-His6	This Study	Addgene 182386
pRSFDuet-1_VNp-mNeongreen	This Study	Addgene 182387
pRSFDuet-1_VNp6-mNeongreen	This Study	Addgene 182388
pRSFDuet-1_VNp15-mNeongreen	This Study	Addgene 182389
pRSFDuet-1_VNp-mNeongreen_OmpA-mCherry	This Study	Addgene 182390
pRSFDuet-1_VNp-mNeongreen_CydAB-mCherry	This Study	Addgene 182391
pETDuet-1_VNp-mCerulean3_Citrine-minD	This Study	Addgene 182420
pRSFDuet-1_VNp-LZ-mNeongreen	This Study	Addgene 182392
pRSFDuet-1_VNp-LZ_CydAB-mNeongreen	This Study	Addgene 182393
pETDuet-1_VenusN154_VenusC155 (BiFC control construct)	This Study	Addgene 87856
pETDuet-1_VNp-VenusN154_VNp-VenusC155 (BiFC construct)	This Study	Addgene 182394

pETDuet-1_VNp-LZ-VenusN154_VNp-LZ-VenusC155 (BiFC construct)	This Study	Addgene 182395
pRSFDuet-1_DARPinOFF7-His_6	This Study	Addgene 182396
pRSFDuet-1_VNp-DARPinOFF7-His_6	This Study	Addgene 182397
pRSFDuet-1_VNp6-DARPinOFF7-His_6	This Study	Addgene 182398
pRSFDuet-1_VNp15-DARPinOFF7 -His_6	This Study	Addgene 182399
pRSFDuet-1_Uricase-His_6	This Study	Addgene 182400
pRSFDuet-1_VNp-Uricase-His_6	This Study	Addgene 182401
pRSFDuet-1_StefinA -His_6	This Study	Addgene 182402
pRSFDuet-1_VNp-StefinA-His_6	This Study	Addgene 182403
pRSFDuet-1_VNp6-StefinA-His_6	This Study	Addgene 182404
pRSFDuet-1_VNp15-StefinA-His_6	This Study	Addgene 182405
pRSFDuet-1_FGF21-His_6	This Study	Addgene 182406
pRSFDuet-1_VNp-FGF21-His_6	This Study	Addgene 182407
pRSFDuet-1_DNAseI-His_6	This Study	Addgene 182408
pRSFDuet-1_VNp-DNAseI-His_6	This Study	Addgene 182409
pRSFDuet-1_hGH-His_6	This Study	Addgene 182410
pRSFDuet-1_VNp-hGH-His_6	This Study	Addgene 182411
pRSFDuet-1_VNp-LZ-hGH-His_6	This Study	Addgene 182412
pRSFDuet-1_mNeongreen	This Study	Addgene 182413
pRSFDuet-1_mNeongreen-DARPinOFF7-His_6	This Study	Addgene 182414
pRSFDuet-1_VNp-mNeongreen-DARPinOFF7-His_6	This Study	Addgene 182415
pRSFDuet-1_mNeongreen-Uricase-His_6	This Study	Addgene 182416
pRSFDuet-1_VNp-mNeongreen-Uricase-His_6	This Study	Addgene 182417
pRSFDuet-1_mNeongreen-StefinA-His_6	This Study	Addgene 182418
pRSFDuet-1_VNp-mNeongreen-StefinA-His_6	This Study	Addgene 182419
pRSFDuet-1_mNeongreen-Etanercept-His_6	This Study	Addgene 182420
pRSFDuet-1_VNp-mNeongreen-Etanercept	This Study	Addgene 182421
pRSFDuet-1_mNeongreen-Erythropoietin-His_6	This Study	Addgene 182422
pRSFDuet-1_VNp-mNeongreen-Erythropoietin -His_6	This Study	Addgene 182423
Software and algorithms		
ImageJ	Schneider et al.	https://imagej.nih.gov/ij/
Compass Data Analysis software	Bruker	
Origin software	OriginLab	
OmniSEC	Malvern	
Metamorph	Molecular Devices	
Zen software	Zeiss	

SPCImage software v.6.9	Becker and Hickl, GmbH	
Other		
Syringe filter, PES, 0.45 μm	Fisherbrand	Cat#15216869
Millipore Express PLUS 0.45μm Membrane	Merck	Cat#HPWP04700

Figure 1

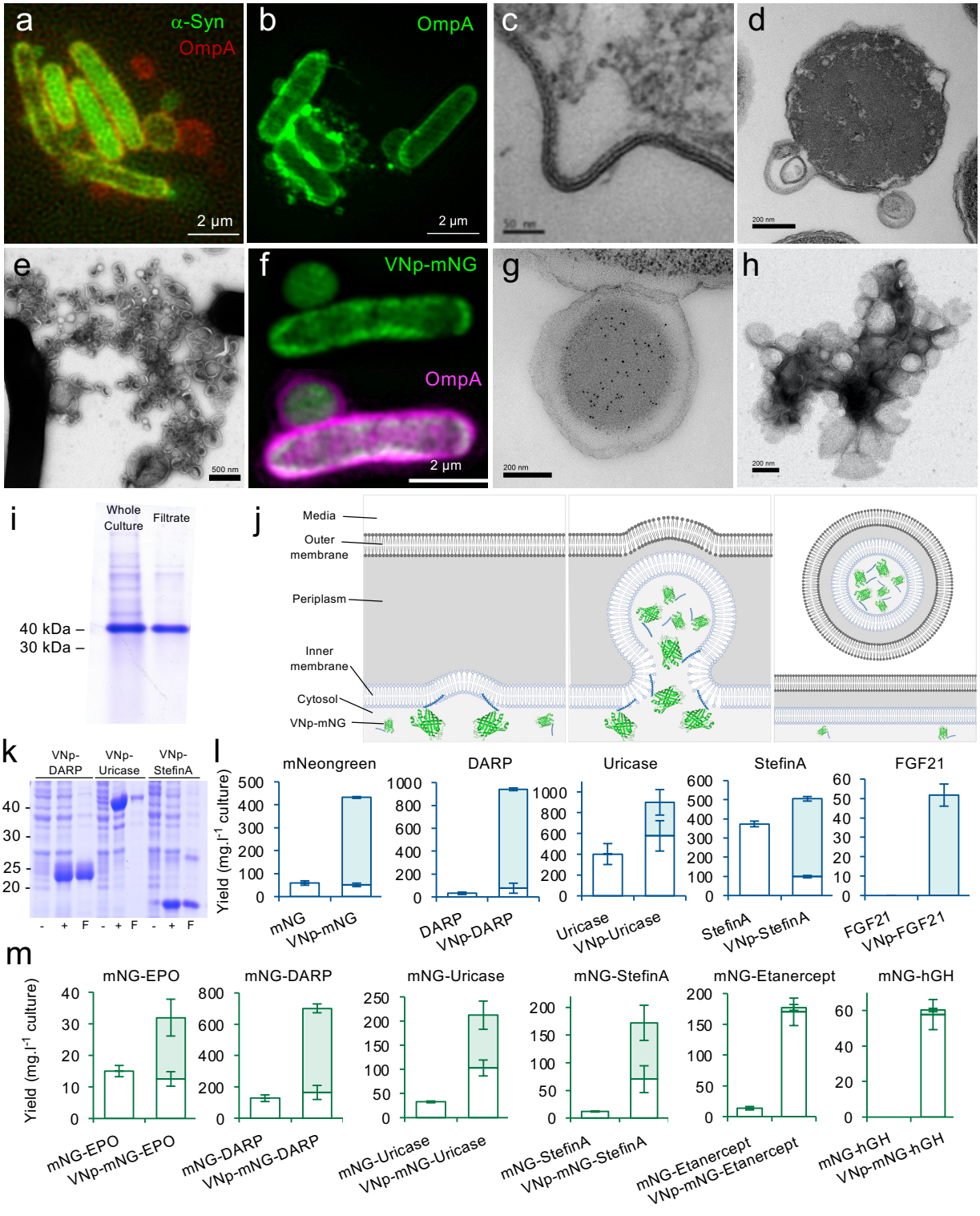
a
α-Syn
OmpA
2 µm
b
OmpA
2 µm
c
d
200 nm
e
500 nm
f
VNp-mNG
OmpA
2 µm
g
200 nm
h
200 nm
i
Whole Culture
Filtrate
40 kDa –
30 kDa –
j
Media
Outer membrane
Periplasm
Inner membrane
Cytosol
VNp-mNG
k
VNp-DARP
VNp-Uricase
VNp-StefinA
40
30
25
20
- + F - + F - + F
l
mNeongreen
DARP
Uricase
StefinA
FGF21
Yield (mg.l-1 culture)
mNG
VNp-mNG
DARP
VNp-DARP
Uricase
VNp-Uricase
StefinA
VNp-StefinA
FGF21
VNp-FGF21
m
mNG-EPO
mNG-DARP
mNG-Uricase
mNG-StefinA
mNG-Etanercept
mNG-hGH
Yield (mg.l-1 culture)
mNG-EPO
VNp-mNG-EPO
mNG-DARP
VNp-mNG-DARP
mNG-Uricase
VNp-mNG-Uricase
mNG-StefinA
VNp-mNG-StefinA
mNG-Etanercept
VNp-mNG-Etanercept
mNG-hGH
VNp-mNG-hGH

Figure 2

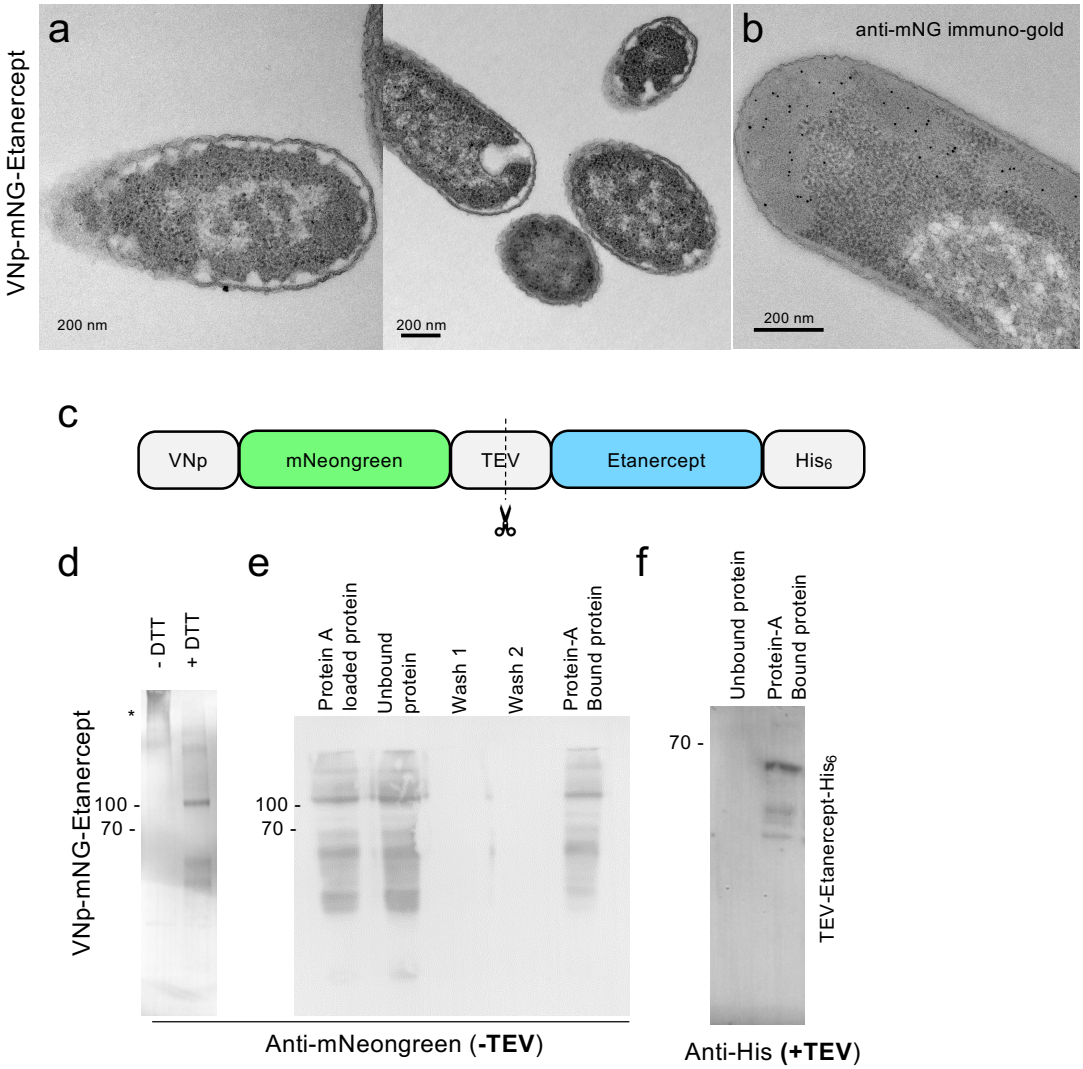
a
b
anti-mNG immuno-gold
VNp-mNG-Etanercept
200 nm
200 nm
200 nm
c
VNp
mNeongreen
TEV
Etanercept
His6
d
- DTT
+ DTT
VNp-mNG-Etanercept
*
100 -
70 -
e
Protein A loaded protein
Unbound protein
Wash 1
Wash 2
Protein-A Bound protein
100 -
70 -
Anti-mNeongreen (-TEV)
f
Unbound protein
Protein-A Bound protein
70 -
TEV-Etanercept-His6
Anti-His (+TEV)

Figure 3

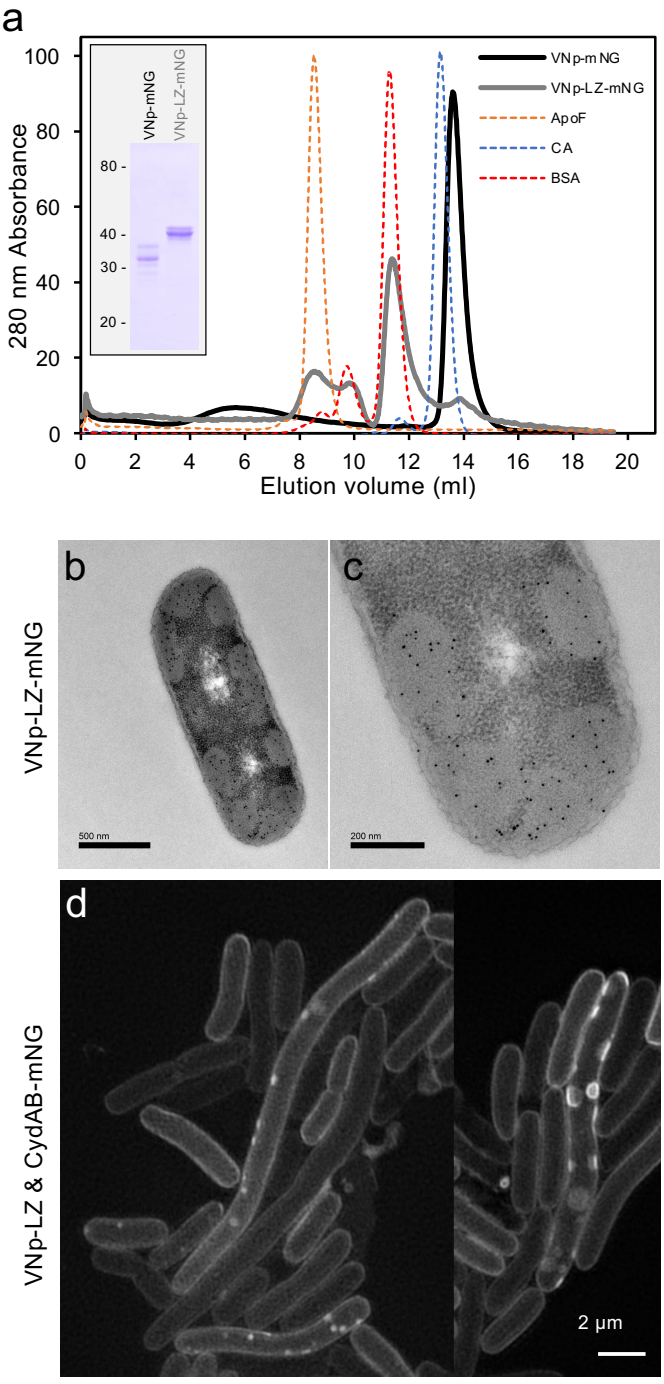
a
280 nm Absorbance
Elution volume (ml)
VNp-mNG
VNp-LZ-mNG
ApoF
CA
BSA
80 -
40 -
30 -
20 -
b
c
500 nm
200 nm
VNp-LZ-mNG
d
VNp-LZ & CydAB-mNG
2 µm